Predictive Braking Algorithm for Soft Starter Driven Induction Motors

Hauke Nannen and Heiko Zatocil
OTH - Technical University of Applied Sciences
Amberg, Germany
h.nannen@oth-aw.de, h.zatocil@oth-aw.de

Gerd Griepentrog
Institute for Power Electronics and Control of Drives
Darmstadt, Germany
gerd.griepentrog@lea.tu-darmstadt.de

Keywords

≪Control of drive≫, ≪Thyristor≫, ≪Induction motor≫, ≪Industrial application≫

Abstract

Different algorithms exist for braking induction motors driven by soft starters. This paper investigates a model predictive algorithm for braking induction motors driven by soft starters in addition to state-of-the-art braking with grid phase rotation. Additionally, the impact of non-linear effects, e.g. saturation and the skin effect, on the predictive algorithm is discussed and evaluated based on simulations and measurements. Measurements of the different braking procedures are presented, compared and discussed. The measurements show that the total losses in the soft starter and the motor can be significantly reduced by the application of the predictive algorithm instead of the conventionally used phase angle control algorithm.

1 Introduction

Direct-on-line induction motors are the common solution for industrial applications with a fixed rotor speed. Besides acceleration and operation of induction motors, the braking of motors can be required. For example, braking is often necessary in applications with high inertia such as circular saws, mills and centrifuges. Without a braking function, the motor would take a lot of time to get to a standstill. Obviously, all these applications can be equipped with mechanical brakes, but this would lead to additional investment, maintenance and a larger construction. Due to these disadvantages, braking features have been discussed in the past [16]. The most prominent braking strategies are braking with DC currents [2, 3, 4, 7], braking with phase rotation [16] and braking using additional capacitors [10, 17]. All these approaches need additional equipment such as electric contactors and rectifiers. When a soft starter is used in the application, several strategies for braking induction motors are possible. Soft starters often use quasi-DC braking or improved braking by a combination of phase rotation and phase angle control.

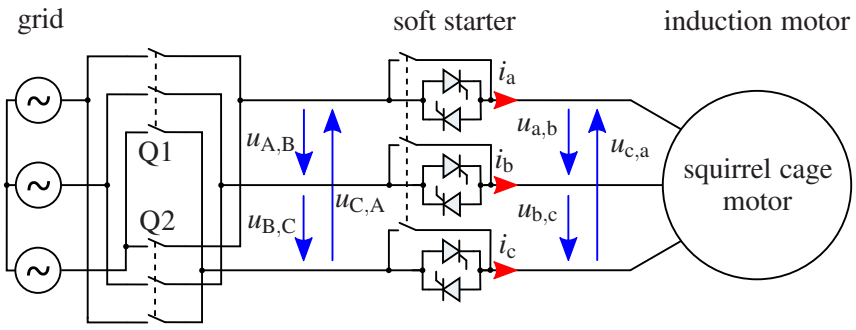

Fig. 1: Soft starter with contactors for inversion of grid rotation direction

Special approaches such as discrete frequency control (DFC) can also be used [6]. Depending on the approach, additional equipment (i.e. contactors) is necessary. Combinations of different algorithms for each time section of the braking procedure often yield the best performance. Nevertheless, all braking strategies have one thing in common: they heat up the motor during braking.

This paper complements the known strategies for braking with a model predictive algorithm, because the major part of the braking power is converted into heat within the electrical machine. In [13] this algorithm approach was used to accelerate a motor. Using this approach leads to a significant loss reduction during start-up, as compared with phase-angle-controlled soft starters. The present paper investigates, whether braking with the predictive algorithm also leads to this loss reduction. Furthermore, the investigations also include a configuration where no additional equipment for braking is necessary.

In the first section of this paper, the state-of-the-art braking procedures for soft starters are presented. The next section presents the prediction algorithm and its modification for braking. Afterwards, the measurements made demonstrate the performance of this approach.

2 State-of-the-Art Braking Strategies

This section presents the state-of-the-art braking strategies for soft starter driven induction motors. As the other approaches are much more common in industrial soft starters, DFC will not be taken into account in the comparison. One way to brake an induction motor is to interchange two phases of the grid. This changes the rotation direction of the grid and the main field in the stator of the motor. Hence, motor slip s changes from $s \approx 0$ to $s \approx 2$. When the motor's speed reaches zero, it is disconnected from the grid. Mostly, the interchange of motor phases is done by contactors or by a set of at least five thyristor pairs.

Using a soft starter can improve the braking. Figure 1 shows a typical configuration of contactors and a soft starter. The contactors Q1 and Q2 are used for changing the rotation direction. After the re-connection with flipped phases, the soft starter performs a phase angle control. This leads to reduced braking currents.

3 Predictive Algorithm

Publications in the recent years have established a predictive algorithm approach for soft starters driving different types of motors [11, 12, 13, 14, 19]. During start-up, these algorithms reduce the losses in the motor and soft starter significantly. The main idea behind these algorithms is to predict the motor torque and current curves for possible firing combinations and to assess their usefulness in an iterative process. The next sections show the theoretical background of these algorithms and adoption for braking.

Motor Model

A motor model is necessary for motor current and torque prediction. A detailed derivation can be found in [13]. Basis for the prediction is a standard induction motor model:

$$L_1 = L_{1\sigma} + L_\mathrm{h} \quad , \quad L_2 = L_{2\sigma} + L_\mathrm{h} \quad , \quad \sigma = 1 - \frac{L_\mathrm{h}^2}{L_1 \cdot L_2} \tag{1}$$

$$\frac{\mathrm{d}\vec{I}_1^\mathrm{S}}{\mathrm{d}t} = \frac{1}{\sigma \cdot L_1} \cdot \vec{U}_1^\mathrm{S} - \frac{R_1 \cdot L_2^2 - R_2 \cdot L_\mathrm{h}^2}{\sigma \cdot L_1 \cdot L_2^2} \cdot \vec{I}_1^\mathrm{S} + \frac{R_2 \cdot L_\mathrm{h}}{\sigma \cdot L_1 \cdot L_2^2} \cdot \vec{\Psi}_2^\mathrm{S} - \mathrm{j} \cdot \frac{\Omega_\mathrm{L} \cdot L_\mathrm{h}}{\sigma \cdot L_1 \cdot L_2} \cdot \vec{\Psi}_2^\mathrm{S} \tag{2}$$

$$\frac{\mathrm{d}\vec{\Psi}_2^\mathrm{S}}{\mathrm{d}t} = \frac{R_2 \cdot L_\mathrm{h}}{L_2} \cdot \vec{I}_1^\mathrm{S} - \frac{R_2}{L_2} \cdot \vec{\Psi}_2^\mathrm{S} + \mathrm{j} \cdot \Omega_\mathrm{L} \cdot \vec{\Psi}_2^\mathrm{S} \tag{3}$$

$$M_\mathrm{M} = \frac{3}{2} \cdot p \cdot \frac{L_\mathrm{h}}{L_2} \cdot \vec{\Psi}_2^\mathrm{S} \times \vec{I}_1^\mathrm{S} \tag{4}$$

The model consisting of Equations (2) – (4) is used for prediction. Before the prediction can be started, the model has to be initialised with the actual system state. The initialisation of the current state $\vec{I}_1^\mathrm{S}$ can be done with the measured currents. As the rotor flux linkage cannot be measured directly with

the soft starter configuration, a flux model is needed for rotor flux estimation. Therefore, Equation (3) is implemented to calculate the actual rotor flux linkage with the measured electric rotor speed Ω_L and stator currents $\vec{I}_1^{\,\mathrm{S}}$.

For solving Equations (2) and (3), a prediction for grid voltage $\vec{U}_1^{\,\mathrm{S}}$ and electric rotor speed Ω_L is also necessary. Therefore, the actual grid voltage can be rotated with the grid frequency f_grid and the prediction sample time t_step. The motor speed can be assumed as being constant due to the high system inertia J_total.

Together with the parameters, the initial and the estimated values, the prediction can be done. Now, the model is used to predict the current and torque over the prediction horizon t_pred. Prediction is done for all four possible firing opportunities (A & B, B & C, C & A, A & B & C) by solving the equations with an Explicit Euler method using a fixed step with t_step. This calculation will be repeated cyclically with new actual values within a defined step with t_cycle. A more detailed explanation can be found in [13].

Decision Criteria

After the motor model-based prediction of the variation over time for the current $\vec{I}_1^{\,\mathrm{S}}$ and the torque M_M for each possible firing opportunity, it is necessary to decide whether the specific firing is useful or not. For braking the motor, it has to obviously generate a negative amount of torque, but some additional aspects must also be taken into account, as discussed in this section.

To brake the motor, the firing needs to generate a minimum amount of negative torque $M_\mathrm{p,avgmin}$ over the prediction horizon t_pred. The absolute torque value $|M_\mathrm{M}|$ is also limited, to prevent the application from damage:

$$\mathrm{mean}\left(M_\mathrm{M}\left(t=0...t_\mathrm{pred}\right)\right) < M_\mathrm{p,avgmin} \quad , \quad |M_\mathrm{M}\left(t=0...t_\mathrm{pred}\right)| > M_\mathrm{p,max} \tag{5}$$

In addition to the torque requirements, it is useful to limit the maximum allowed peak current $i_\mathrm{p,max}$, as well as the minimum allowed conduction time $t_\mathrm{p,mc}$. This makes the system more robust, and firings with a small amount of torque are suppressed. Finally, a criterion for managing the rotor flux linkage is necessary. Without a significant rotor flux linkage amplitude $|\vec{\Psi}_2^{\mathrm{S}}|$, no torque can be created afterwards. This necessitates the setting of a limit on the rotor flux $\Psi_\mathrm{p,min}$, which must be still available at the end of each firing:

$$|\vec{I}_1^{\,\mathrm{S}}\left(t=0...t_\mathrm{pred}\right)| < i_\mathrm{p,max} \quad , \quad t_\mathrm{pred} > t_\mathrm{p,mc} \quad , \quad |\vec{\Psi}_2^{\mathrm{S}}\left(t=t_\mathrm{pred}\right)| > \Psi_\mathrm{p,min} \tag{6}$$

When one of the predicted firing opportunities fulfills the requirements of Equations (5) and (6), the respective firing will be initiated on the real hardware. This creates a firing pattern that is more or less equal to the predicted one and considers the rotor flux. The main difference is that all other known braking strategies are based on fixed pulse patterns. Thus, in the predictive algorithm, firing is only applied to the system when a requested torque is produced, and the resulting rotor flux linkage at the end is within a limitation.

4 Impact of Non-Linear Effects

The motor model, which is described by Equations (1) – (4), deals with constant motor parameters. In reality, non-linear effects such as the saturation of the magnetic material, skin effect in the rotor bars and resistance variations due to temperature variations of the stator and/or rotor winding may occur. As these effects are not covered by the motor model used by the predictive algorithm, the predicted variations of stator current and torque might vary from the actual ones. The impact of these effects is examined in the next sections.

Saturation

Generally, two saturation effects can be observed in induction motors: the saturation of the main flux paths, resulting in a decreasing main inductance, and the saturation of the leakage flux paths, which leads to varying leakage inductances.

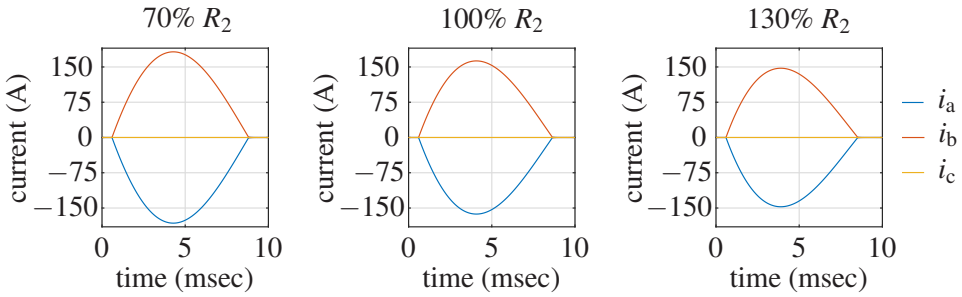

Fig. 2: Simulated variation of rotor resistance at $n = 1050\,\text{rpm}$ with no magnetisation

Induction motors used in industrial applications typically have a rotor time constant higher than 100 ms.

$$\tau_{\text{rot}} = \frac{L_2}{R_2} \tag{7}$$

In contrast to that, a single stator current pulse only lasts for a few 10 ms. Thus, this short current pulse has only a small impact on the main magnetisation level of the motor. Additionally, the rotor flux level $|\vec{\Psi}_2^{\text{S}}|$ is controlled to a defined level and will not exceed a certain reasonable level. Consequently, the saturation of the main flux can be neglected during the prediction of the motor currents and torque. For motors with distinct saturation phenomena during a single pulse, the resulting behaviour of the main inductance can be characterised and integrated into the motor model, according to [9].

As shown in [8], an analytical description of the saturation of the leakage paths is quite impossible. The resulting saturation behaviour severely depends on the geometry of the motor and a lot of other attributes. Some parts of the leakage paths saturate (e.g. the face side leakage paths), while some do not. In [15] one component of leakage saturation effects is described analytically, but not the whole resulting effect.

Skin Effect

During the operation of a soft starter, the skin effect in the rotor cage can be generated in two ways. First, it occurs during steady state operation with high slip values. As shown later, while applying the predictive algorithm, the stator currents during the start-up of the motor have a non-sinusoidal form. Thus, during this operation mode as well, skin effects occur in the rotor, as the non-sinusoidal currents also consist of high frequency components. In both cases, the skin effect leads to an increase in rotor resistance R_2 as the rotor currents are pushed to the upper part of the rotor slots. For the same reason, the rotor leakage inductance $L_{2\sigma}$ decreases simultaneously.

Figure 2 shows the simulation results for a single stator current pulse for different values of R_2 while all other motor parameters were kept constant. Obviously, even huge variations in rotor resistance have no severe impact on the magnitude and variation in stator currents. Nevertheless, the skin effect influences the produced torque as well as the resulting stator currents. If this impact cannot be neglected, it can be integrated in the motor model [1, 5, 18].

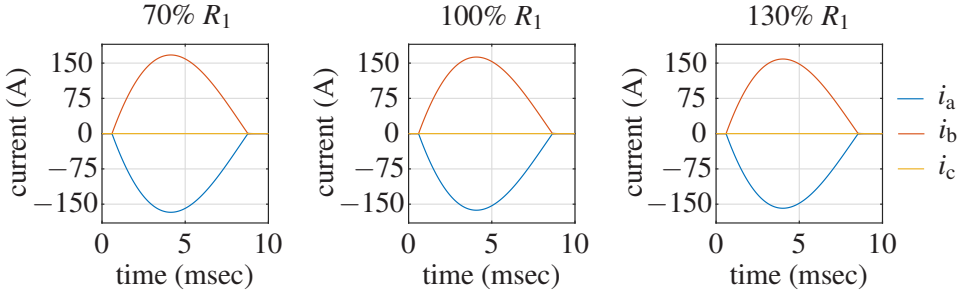

Fig. 3: Simulated variation of stator resistance at $n = 1050\,\text{rpm}$ with no magnetisation

Temperature

In addition to saturation and the skin effect, temperature variations also lead to time-varying motor parameters, especially stator and rotor resistance. The impact of a rotor resistance variation on the resulting stator current pulse is already shown in Figure 2. Figure 3 shows the resulting stator current pulse for three different values of the stator resistance. As expected, the current shapes differ, but the differences are minimal.

Resulting Prediction Error

As shown above, all three non-linear phenomena affect the produced torque and the stator currents. Figure 4 shows the predicted and the real motor currents over a few current pulses during a motor start-up on the test bench. Obviously, the differences between the predicted and the measured motor currents are small and in a reasonable range. The general current shapes and magnitudes are predicted with good precision.

In industrial applications the current and the speed are controlled by dedicated controllers. Additionally, these controllers compensate the impact of possible prediction errors so that these errors do not disturb the resulting system behaviour.

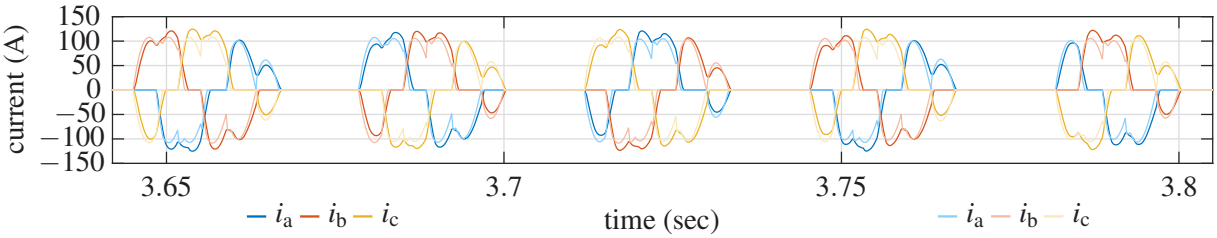

Fig. 4: Exemplary comparison of the predicted current (lighter colour) and the measured current (full colour)

5 Experimental Results

For the comparison of the state-of-the-art and the predictive braking approach with a focus on the losses in the motor and the soft starter, it is necessary to define, measure and calculate the dissipated energy.

The two important values for a loss comparison are the dissipated energy in the motor E_{mot} and that within the soft starter E_{thy} during braking. They limit the number of starts and stops per hour. The overall electrical energy consumption E_{elec} during braking is measured with a power analyser between the motor and the soft starter. Together with the energy stored in the rotating mass E_{mech} and the dissipated energy due to friction E_{fric}, the dissipated energy in the motor E_{mot} can be calculated:

$$E_{\text{mot}} = E_{\text{elec}} + \Delta E_{\text{mech}} - E_{\text{fric}} \tag{8}$$

ΔE_{mech} represents the difference in mechanical energy stored in the rotating mass. The mechanical energy in the rotating mass can be calculated with the system inertia J_{total} and the current rotor speed n as follows:

$$E_{\text{mech}} = 1/2 \cdot J_{\text{total}} \cdot (2\pi \cdot n)^2 \tag{9}$$

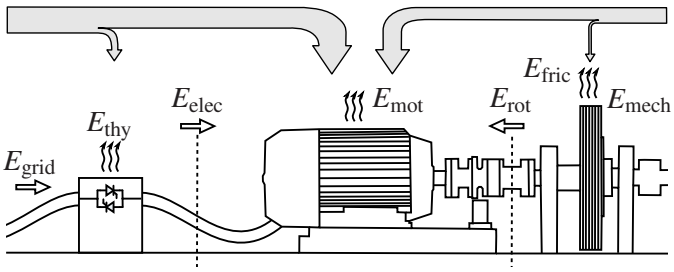

Fig. 5: Energy flow during braking

When the motor is stopped, all the energy of the rotating mass is transformed by the motor into electrical energy or heat. The dissipated energy within the soft starter E_{thy}, can be calculated based on the measured

currents and a simple loss model with forward voltage U_f and dynamic resistance R_{on}:

$$E_{thy} = \int_{t_{start}}^{t_{stop}} U_f \cdot (|i_a| + |i_b| + |i_c|) + R_{on} \cdot (i_a^2 + i_b^2 + i_c^2) dt \tag{10}$$

When the first current pulse for braking is done, the braking begins at t_{start} and ends at t_{stop}, when the motor is stopped.

Figure 5 shows the energy flow in the system during braking. E_{grid} is defined as energy consumption from grid, and E_{rot} is the amount of energy that is transferred from the rotating mass into the motor. To measure the dissipated energy due to friction, the motor was coasted to a standstill. The measurements showed that the mechanic losses E_{fric} are neglectable on this test bench.

Experimental Setup

The main parts of the used test setup are shown in Figure 5. Central elements are a standard industrial induction motor for direct line-start, contactors for phase rotation and a soft starter. They are connected as shown in Figure 1. The induction motor is connected to a speed sensor and a mechanical unit. With this mechanical unit additional inertia can be added to the rotor shaft using disks. With these disks, the system inertia J_{total} can be adjusted. All the shown data are measured with a high-precision power analyser LMG671 from ZES ZIMMER. The algorithms for controlling the thyristors are implemented on a dSPACE rapid controller prototyping system (RCP-system).

Regarding the braking time, the parameters of the algorithms were chosen in such a way that the total braking times for both algorithms could be compared. As the resulting braking time for the predictive algorithm depends on its parameters, a general comparison with an explicit result is difficult.

Phase Angle Control Algorithm

In Figure 6 a braking with phase rotation and phase angle control is shown. The procedure starts with a motor, which is connected to the grid via bypass and runs in steady state. First, contactor Q1 and the bypass contactor are opened, and then the motor runs for a short time without grid connection. Afterwards, contactor Q2 is closed, and the soft starter starts with phase angle control in the opposite direction, until the rotor is stopped. Figure 6 shows the current shape for phase angle control, which is well known, and continuous speed reduction.

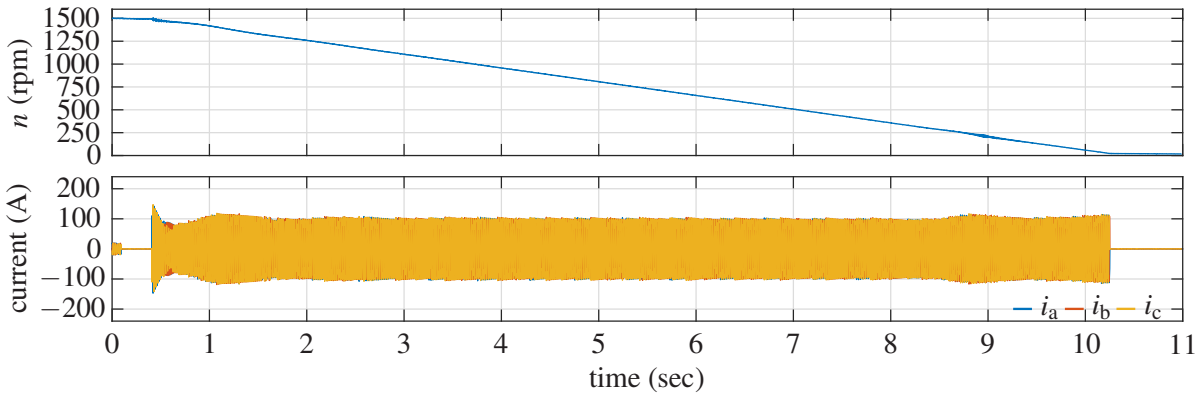

Fig. 6: Braking with phase rotation and phase angle control for current reduction

Predictive Algorithm

The predictive approach does not use any additional contactors, only a pure soft starter. Thus, the soft starter can only create braking torque by connecting the stator windings to a grid that voltage space vector rotates in the same direction as the rotor flux linkage.

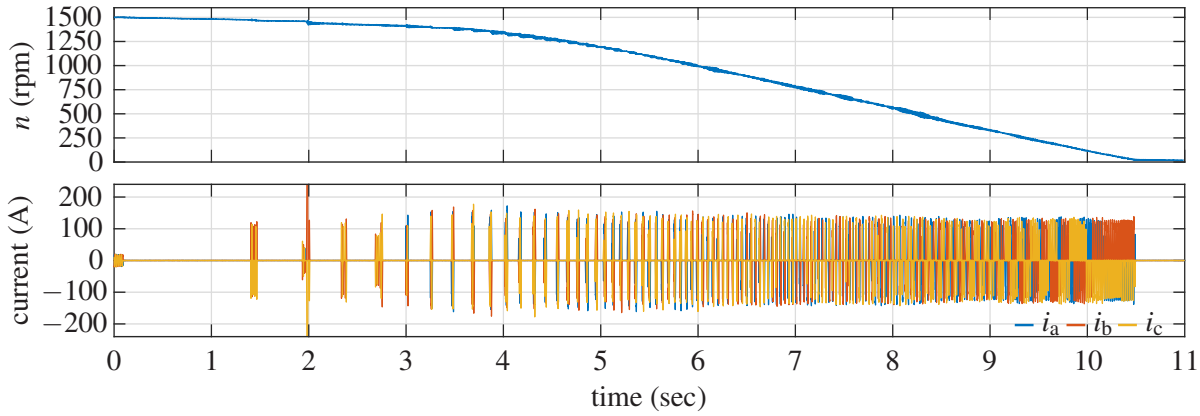

Fig. 7: Braking with predictive algorithm and without phase change

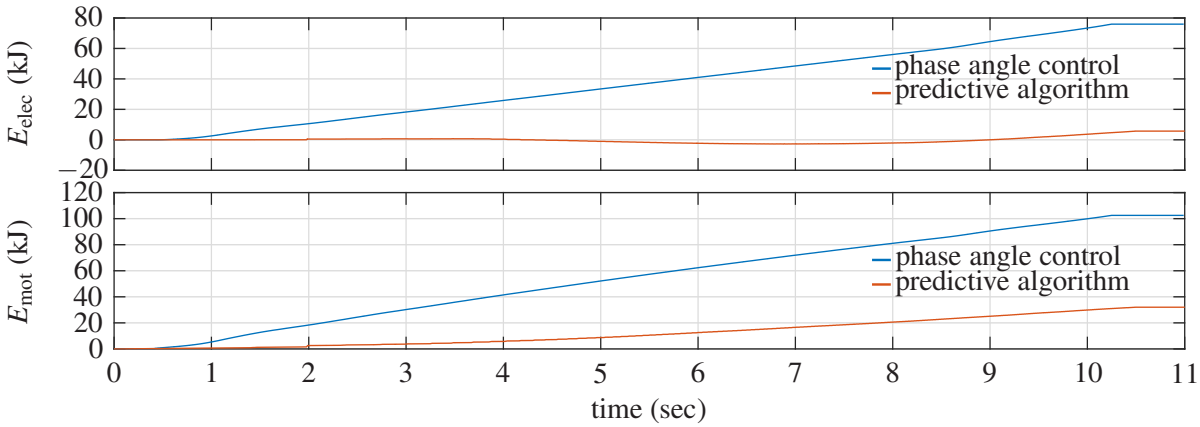

Fig. 8: Comparison of the accumulated energy flow during braking

Figure 7 shows that the braking consists of two time phases. In the first part, the algorithm leads to a kind of current burst mode. The current flows in short intervals, which are divided by time spent without current. This time decreases with every period until the second phase of braking starts, which features continuous braking. In the end of the second phase, the rotor is stopped.

In the first phase, the braking torque is less than in the second phase. This is the consequence of the large time periods without current in the first phase. The reason is the equal direction and nearly equal rotation speed of the grid and the motor, which leads to fewer opportunities for negative torque creation.

Comparison

Previous investigations have shown that the losses during start-up can be lowered by using a predictive algorithm for firing pulse generation [13]. This is investigated for braking.
In Figure 8, the energy flow during braking is shown. In the upper diagram, the electrical energy consumed from the power supply is shown.

The diagram also indicates that the phase angle control algorithm needs electrical energy from the net during the whole braking process. Although negative torque is generated by the motor, the converted energy is not transferred from the rotor to the stator but transformed to ohmic losses directly in the rotor. In contrast the predictive algorithm needs, in sum, nearly no electrical energy from the power supply during braking. This is because the motor works in real generator mode while using the predictive algorithm and, as a consequence, converts mechanical energy to electrical energy in the rotor and transforms this energy from the rotor to the stator winding. This transformed energy is used in the stator to, e.g. supply the stator losses.

The lower diagram in Figure 8 shows the overall motor losses during braking. The comparison between the two control approaches shows that the application of the predictive algorithm can help tremendously decrease the total motor losses, as the algorithm does not utilise a continuous current flow but a discrete one, which lowers the stator losses.

Figure 9 shows the calculated dissipated energy (Equation (8) and (10)) in the motor and the soft starter obtained from the measurements shown in Figures 6 and 7. Motor losses decrease by around 65 % when using the predictive approach. Thus the thermal stress for the motor reduces significantly.

Comparing the predictive algorithm approaches with the phase rotation braking, the losses in the thyristors can be reduced by 50 %, depending on which values are compared. Due to this significant loss reduction, the same soft starter can stop even larger motors or can perform more starts and stops per hour.

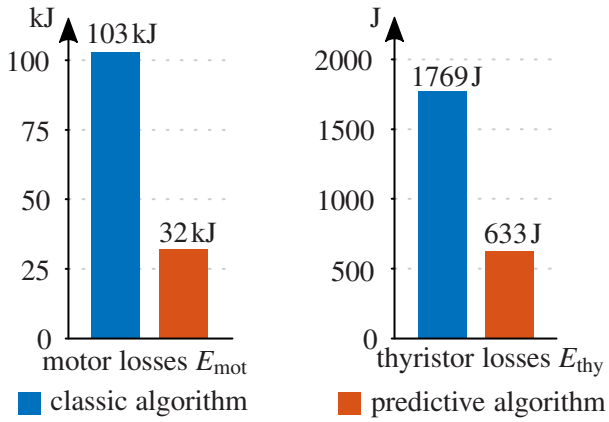

Fig. 9: Thyristor and motor losses during braking

6 Conclusion

This paper investigates different braking procedures for soft starter-driven induction motors. In addition to opposite phase rotation braking, the predictive approach is presented. The measurement results achieved on the test bench demonstrate that the losses in the motor can be lowered significantly. With these approaches, it is possible to stop the motor much more often without damaging it because of overtemperature. The presented measurements show that braking with soft starters is also possible without any additional contactors for phase reversal. This can significantly reduce the system costs for industrial realisations. The losses in the soft starter are shown to be reduced significantly by using the predictive approach. This enables more starts and stops per hour with the same soft starter, or the same soft starter can be used to stop even larger motors.

References

[1] M. Benecke, R. Doebbelin, G. Griepentrog, and A. Lindemann. *Skin Effect in Squirrel Cage Rotor Bars and Its Consideration in Simulation of Non-steady-state Operation of Induction Machines: Progress in electromagnetics research symposium March 20-23, 2011 Marrakesh, Morocco ; proceedings*. The Electromagnetics Academy, Cambridge, Mass., 2011.

[2] O. I. Butler. Stopping time and energy loss or a-c motors with d-c braking. *Transactions of the American Institute of Electrical Engineers. Part III: Power Apparatus and Systems*, 76(3):285–290, 1957.

[3] O. I. Butler and M. N. Abdel-Hamid. D-c dynamic braking of double-cage induction motors. *Transactions of the American Institute of Electrical Engineers. Part III: Power Apparatus and Systems*, 77(3):1035–1038, 1958.

[4] C. F. Evert. Dynamic braking of squirrel-cage induction motors [includes discussion]. *Transactions of the American Institute of Electrical Engineers. Part III: Power Apparatus and Systems*, 73(2):242–244, 1954.

[5] G. Huth. Description of transient deep bar effect with numerical defiend equivalent circuits (in german). *Archiv für Elektrotechnik*, 70(1):31–37, 1987.

[6] M. Laabidi, B. Rebhi, F. Kourda, M. Elleuch, and L. Ghodbani. Braking of induction motor with the technique of discrete frequency control. In *2010 7th International Multi- Conference on Systems, Signals and Devices*, pages 1–6, 2010.

[7] W. A. Lapierre and N. Metaxas. D-c dynamic braking of induction motors. *Electrical Engineering*, 72(9):785, 1953.

[8] T. A. Lipo and A. Consoli. Modeling and simulation of induction motors with saturable leakage reactances. *IEEE Transactions on Industry Applications*, IA-20(1):180–189, 1984.

[9] G. Müller, K. Vogt, and B. Ponick. *Calculation of Electrical Machines (in German)*, volume 2 of *Electrical Machines*. Wiley-VCH, Weinheim, 6. edition, 2009.

[10] S. S. Murthy, G. J. Berg, C. S. Jha, and A. K. Tandon. A novel method of multistage dynamic braking of three-phase induction motors. *IEEE Transactions on Industry Applications*, IA-20(2):328–334, 1984.

[11] H. Nannen and H. Zatocil. Initial rotor position determination of a soft starter driven synchronous motor. In *PCIM Europe 2017; International Exhibition and Conference for Power Electronics, Intelligent Motion, Renewable Energy and Energy Management*, pages 1–6, 2017.

[12] H. Nannen and H. Zatocil. Sensorless start-up of soft starter driven line-start pmsm based on back emf measurement. In *2017 IEEE 26th International Symposium on Industrial Electronics (ISIE)*, pages 354–361, 2017.

[13] H. Nannen, H. Zatocil, and G. Griepentrog. Novel predictive start-up algorithm for soft starter driven induction motors. In *IECON 2020 The 46th Annual Conference of the IEEE Industrial Electronics Society*, pages 3071–3078, 2020.

[14] H. Nannen, H. Zatocil, and G. Griepentrog. Predictive firing algorithm for soft starter driven induction motors. *IEEE Transactions on Industrial Electronics (Early Access)*, 2022.

[15] H. M. Norman. Induction motor locked saturation curves. *Electrical Engineering*, 53(4):536–541, 1934.

[16] H. C. Specht. Electric braking of induction motors. *Proceedings of the American Institute of Electrical Engineers*, 31(5):583–596, 1912.

[17] A. K. Tandon, S. S. Murthy, and B. P. Singh. Experimental studies on a novel braking system for induction motors. *IEEE Transactions on Industry Applications*, IA-20(5):1238–1243, 1984.

[18] P. Vas. *Sensorless Vector and Direct Torque Control*, volume 42 of *Oxford Science Publications*. Oxford [u.a.], reprinted. edition, 2003.

[19] H. Zatocil and H. Nannen. Sensorless start-up of soft starter driven ie4 motors. In *2017 19th European Conference on Power Electronics and Applications (EPE'17 ECCE Europe)*, pages 1–9, 2017.